

COMMISSIONING THE DARHT-II SCALED ACCELERATOR*

Carl Ekdahl[#], E. O. Abeyta, P. Aragon, R. Archuleta, R. Bartsch, D. Dalmas, S. Eversole, R. Gallegos, J. Harrison, J. Johnson, E. Jacquez, B. Trent McCuistian, N. Montoya, S. Nath, D. Oro, L. Rowton, M. Sanchez, R. Scarpetti, M. Schauer, and G. Seitz,
Los Alamos National Laboratory, Los Alamos, NM 87545, USA

H. Bender, W. Broste, C. Carlson, D. Frayer, D. Johnson, A. Tipton, and C. Y. Tom,
Bechtel Nevada, Los Alamos, NM 87544, USA

and M. Schulze,
SAIC, San Diego, CA 92121, USA

Abstract

When completed, the DARHT-II accelerator will produce a 2-kA, 17-MeV beam in a 1600-ns pulse. After exiting the accelerator, the long pulse will be sliced into four short pulses by a kicker and quadrupole septum and then transported for several meters to a tantalum target for conversion to bremsstrahlung for radiography[1]. In order to provide early tests of the kicker, septum, transport, and multi-pulse converter target we assembled a short accelerator from the first available refurbished cells, which are now capable of operating of operating at over 200 kV [2]. This scaled accelerator was operated at ~ 8 MeV and ~1 kA, which provides a beam with approximately the same beam dynamics in the downstream transport as the final 17-MeV, 2-kA beam.

INTRODUCTION

In March, 2006 we began operation of an accelerator designed to provide the beam for early tests of the DARHT-II kicker, downstream transport, and multi-pulse target. Although all of these components were tested at LLNL using the 50-ns, 5-MeV, 1-kA ETA accelerator [3], they had never been tested with a beam long enough for the kicker to produce realistic multiple pulses at the target. The multi-pulse target performance was considered to be a significant physics risk, so we used the first available refurbished cells to construct a short accelerator with energy scaled down to be comparable to ETA. The objective was to use the 1600-ns long beam produced by this “scaled accelerator” to demonstrate performance of the kicker, which would then provide four pulses on the target with energy deposition comparable to that expected from the final 18-MeV accelerator. Another objective was to provide early operational experience with the refurbished cells at > 200 kV/cell.

Before beginning operation we installed ferrites in the injector high-voltage column to damp the 7.8-MHz LC oscillations on the diode waveform [4]. We also installed a new dispenser cathode and apertures in the beam-head

cleanup zone (BCUZ).

We operated the injector diode at 2.1 MV to provide ~1-kA of space-charge limited current for the scaled accelerator, which was constructed from 6 legacy injector cells and the first 26 available refurbished cells. This configuration enabled us to produce a beam with a 1600-ns long “flat-top” and accelerate it to 8 MeV.

The choice of beam current was dictated by the scaling of beam transport to the full-scale 18-MeV accelerator. The beam envelope equation provided our guidance for this:

$$\frac{d^2R}{dz^2} = -k_\beta^2 R + \frac{2I_b}{I_A (\gamma\beta)^2 R} + \frac{\epsilon_n^2}{(\gamma\beta)^2 R^3}$$

where $k_\beta = 2\pi B/I_A$ and $I_A = 17\beta\gamma$ kA. Noting that the ratio of de-focusing terms is proportional to $v/\gamma = I_b/I_A$ (the Budker parameter) suggests using v/γ to establish the scaling of beam dynamics from 18 MeV down to 8 MeV. Based on this scaling, the ideal current at 8-MeV would be 0.92 kA to have dynamics similar to an 18-MeV, 2-kA beam.

We followed our usual procedure to design the tunes for the scaled accelerator, using our XTR envelope code with initial conditions from TRAK ray-trace and LSP PIC simulations of the diode [4]. All of the tunes use the first two or three cell blocks to compress the beam to the small matched radius resulting from the strong transport field required to suppress the beam breakup (BBU) instability [5].

We completed commissioning the scaled accelerator in June, 2006, and the accelerator was then used until February, 2007 for the kicker and multipulse-target tests [6]. In this article we describe the long-pulse beam measurements made during commissioning.

BEAM-PARAMETER MEASUREMENTS

DARHT-II is heavily instrumented for beam parameter measurements. Beam position monitors (BPMs) based on measurements of the beam-produced magnetic field are located throughout the injector and accelerator. A magnetic-dipole spectrometer is used for measuring the electron kinetic energy. Fast gated intensified-CCD

*Work supported by the US National Nuclear Security Agency and the US Department of Energy under contract W-7405-ENG-36.

[#]cekdahl@lanl.gov

cameras record snapshots of the beam profile produced by Cerenkov light from fused-silica targets, and time resolved profiles are tomographically reconstructed from 4-view streak camera images of these targets.

Beam Current and Motion

The scaled-accelerator BPMs were the same as used in all DARHT-II tests since the accelerator was first operated in 2002[4]. With calibration, the uncertainty in our BPM measurements of beam position, current, and quadrupole moment is limited by our data recording digitizers to $\pm 0.5\%$ for beams near the axis. A total of 13 BPMs were installed, producing 195 channels of digitally recorded data. These were located at the entrance to each block of 6-8 cells, at the exit of the diode, at the exit of the accelerator, and at the beam-imaging station 3.5-m downstream of the accelerator exit.

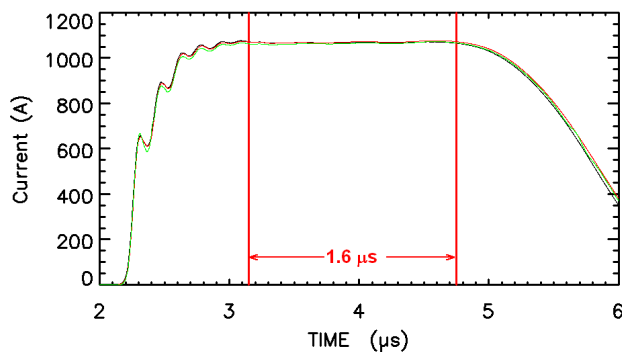


Figure 1: Overlay of current measured by four injector BPMs -- in the diode anode, and injector cell-block entrance and exit. The current was constant to within $\pm 0.5\%$ over the 1.6- μs flat-top indicated by the red markers.

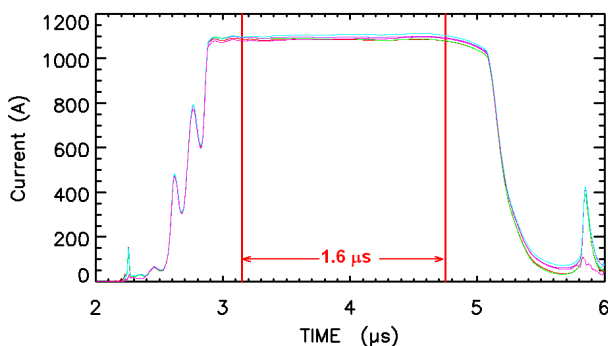


Figure 2: Overlay of current measured by five accelerator BPMs -- at the entrance to each cell block, and at the accelerator exit. The current was constant to within $\pm 0.5\%$ over the 1.6- μs flat-top indicated by the red markers.

Figure 1. shows the current through the injector cell block. The BPM-to-BPM rms variation of average flat-top current was $< 1\%$. Figure 2. shows the current after passing through the BCUZ into the accelerator. This clearly shows the loss of off-energy head and tail in the BCUZ. Again, the BPM-to-BPM rms variation of average

flat-top current was $< 1\%$, showing that beam loss in the accelerator, if any, is less than our measurement capabilities at this time.

The beam motion during the 1.6- μs measured with a BPM at the accelerator exit is shown in Figure 3. This motion is much less than the beam size predicted at this position by our XTR envelope code (illustrated in red). (For size reference, the beam pipe transitions from the 250-mm diameter in the accelerator down to the 150-mm diameter of the downstream sections at this location.)

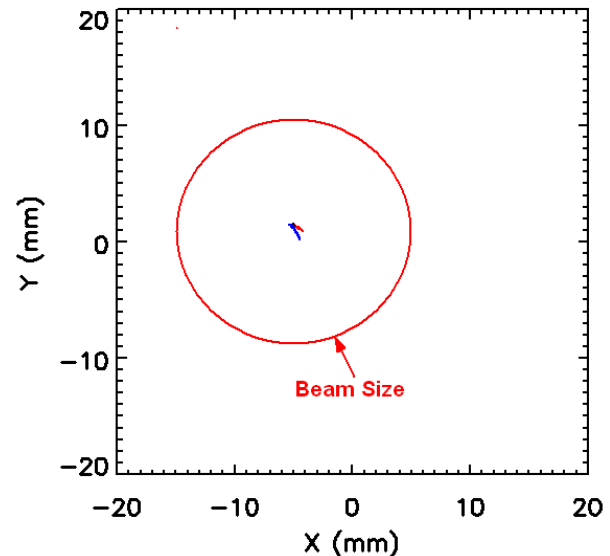


Figure 3: Beam motion at the accelerator exit compared with the beam size predicted by envelope code.

Beam Energy

The time-resolved electron kinetic energy was measured with a 60° magnetic-dipole spectrometer with a streak-camera readout of a scintillator in the imaging plane. This magnetic spectrometer has been in use since 1990 to measure electron kinetic energy on the ITS, ETA, FXR, DARHT-I, and DARHT-II accelerators. Within the past few years it has been upgraded with a modern power supply having 0.005% current regulation and recalibrated using a 3-keV to 50-keV negative ion accelerator specifically designed for this purpose. The present calibration from 2 MeV/c to 20 MeV/c is within $\pm 0.5\%$ absolute.

Using this spectrometer, we measured the beam energy at the scaled accelerator exit to be 8.02 MeV $\pm 0.65\%$ over the 1.6- μs flat-top region of the pulse (Figure 4).

Beam Emittance, Size, and Divergence

To estimate the beam emittance, size, and divergence at the accelerator exit we used a single focusing solenoid to vary the beam size at the Cerenkov imaging target. We then found the most likely parameters at the accelerator exit by fitting the measured beam size to XTR envelope code predictions. The beam size measurements were obtained using a four-view streak camera with quasi-anamorphic optics to circumvent the need for a slit [7]. Beam sizes were obtained at seven different times during

the flat-top of the pulse, so the statistics of the fit (shown in Figure 5) includes the variation of the beam parameters during the 1.6- μ s flat-top.

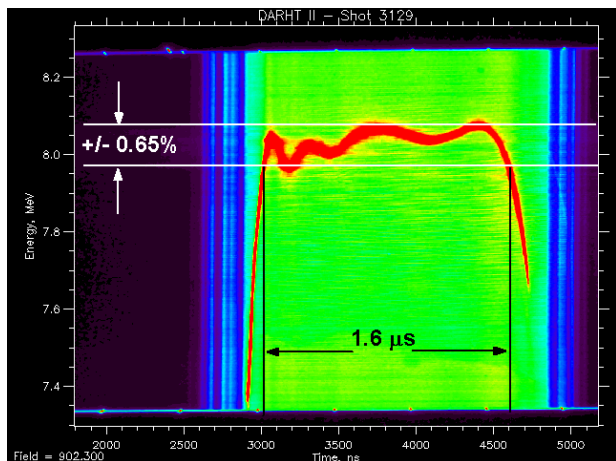


Figure 4: Time-resolved electron kinetic energy measured by our magnetic spectrometer, showing that the energy variation over the 1.6- μ s flat-top is less than $\pm 1\%$.

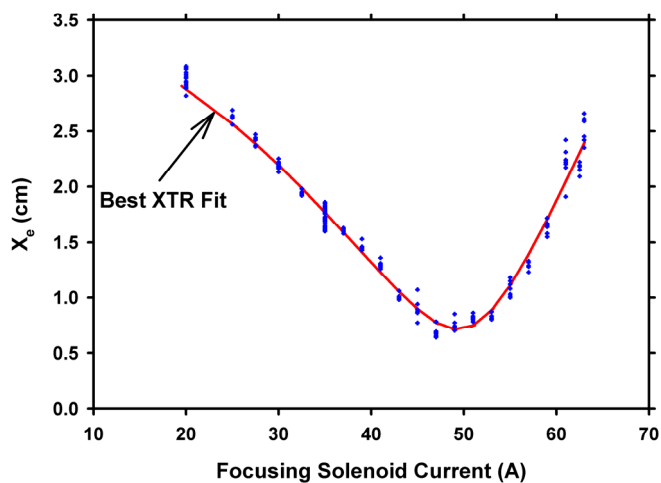


Figure 5: XTR envelope code fit to 182 beam size measurements obtained from the 4-view streak camera.

The technique of fitting XTR envelope simulations to a focusing-magnet scan was a particularly meaningful way of determining beam parameters at the accelerator exit, because the same envelope model was to be used with these exit parameters as initial conditions for tuning the downstream and final focus [6]. The best fit of the beam exit parameters from XTR envelope simulations are given in Table 1, along with the measured beam energy and current.

SUMMARY

We installed and commissioned an 8-MeV scaled accelerator in order to test the critical downstream

systems required for producing multiple radiography pulses. During commissioning of this accelerator we measured the beam parameters needed for tuning the kicker, downstream transport and final focus (see Table I). Uncertainties in these measurements were within the bounds of the acceptance of the downstream components. This accelerator subsequently provided more than 1,000 long-pulse beam shots for tests of the downstream components [6].

Table I. Beam parameters at exit of scaled accelerator

Parameter		Units	Value	
Energy	KE	MeV	8.02	$\pm 0.5\%$
Current	I_b	kA	0.9-1.1	$\pm 2\%$
Radius	R_0	cm	0.8	$\pm 3\%$
Divergence	R_0'	mr	3.2	$\pm 16\%$
Normalized Emittance	ϵ_n	π -mm-mr	617	$\pm 10\%$

REFERENCES

- [1] "Status of the DARHT Phase 2 Long-Pulse Accelerator," M. J. Burns, et al., PAC2001, Chicago, IL, 2001, p. 325.
- [2] R. Scarpetti, et al., "Status of the DARHT 2nd axis at Los Alamos National Laboratory," IEEE Pulsed Power Conference, Monterey, CA, 2005, pp 37-42.
- [3] Yu-Jiuan Chen, et al., "Downstream system for the second axis of the DARHT facility," LINAC 2002, Gyeongju, Korea, 2002, pp. 16-20.
- [4] Carl Ekdahl, et al., "Initial electron-beam results from the DARHT-II linear induction accelerator," IEEE Trans. Plasma Sci., vol. 33, 2005, pp. 892-900.
- [5] Carl Ekdahl, et al., "Long-pulse beam stability experiments on the DARHT-II linear induction accelerator," IEEE Trans. Plasma Sci., vol 34, 2006, pp.460-466.
- [6] Martin E. Schulze, et al., "Commissioning the DARHT-II scaled accelerator downstream transport," PAC07, Albuquerque, NM, 2007.
- [7] H. Bender, et al., "Quasianamorphic optical imaging system with tomographic reconstruction for electron beam imaging," Rev. Sci. Instrum., vol. 78, 2007, p 013301.